Reversible Raman D-band changes: A new probe into the pressure-induced collapse of carbon nanotubes

R. Galafassi, F. Vialla, V. Pischedda, H. Diaf, A. San-Miguel

Reversible Raman D-band changes: a new probe into the pressure-induced collapse of carbon nanotubes

R. Galafassi[a], F. Vialla[a], V. Pischedda[a], H. Diaf[a], A. San-Miguel[a,*]

[a]*Université Claude Bernard Lyon 1, CNRS, Institut Lumière Matière UMR 5306, F-69622, Villeurbanne, France*

Abstract

The control of the geometry of carbon nanotubes has a high potential for electro-optical technology developments. We report here the use of a new spectroscopic signature for the detection and characterization of the pressure induced radial buckling of single walled carbon nanotubes using Raman spectroscopy combined with sapphire anvil cell pressure systems. We follow the appearance of a defect-free Raman D-band contribution in bundled samples which is assigned to the pressure-induced radial buckling, as already shown on radially collapsed nanotubes at ambient pressure. On pressure release, this contribution to the D-band disappears, confirming the reversibility of the process. We applied this approach to the study of isolated tubes and followed the collapse transition of a 1.7 nm diameter tube, most likely identified as a (16,8) chirality, starting at 1 GPa and ending at 2 GPa. Our study further illustrates the potential of utilizing the D-band as a new spectroscopic probe to explore geometrical changes in carbon nanotubes.

Keywords: Carbon nanotube, high pressure, Raman spectroscopy, D-band, strain engineering, collapsed nanotube, sapphire anvil cell

1. Introduction

The actual geometrical shape of carbon nanotubes (CNT) strongly influences their effective properties, in particular the electronic and optical ones, and thus introduces an interesting mean for fine-tuning towards applications [1, 2, 3, 4, 5, 6, 7]. The geometry of carbon nanotubes can be affected by many different intrinsic factors, such as their diameter, number of walls, or the presence of defects, as well as external factors, such as charge injection or pressure application [8]. When subjected to high pressure, many investigations have predicted the evolution of carbon nanotube geometrical cross-section through other geometries than circular including oval, collapsed with two or even more lobes [9, 10, 11, 12]. Experimentally, the transition to different collapsed geometries has been evidenced by a number of studies [13, 14, 15, 16, 17, 18, 19] and a complete phase-diagram providing the limits of the circular cross-section geometry as a function of the diameter and the number of tube walls has been proposed [8]. The two extreme states, circular and collapsed, of the nanotube cross-section offer interesting opportunities for the control of many physical properties [17, 20, 2]. These opportunities can be significantly expanded by introducing a continuous control of states between those limits. This may be reached, for instance, through the endohedral filling of carbon nanotubes with different atoms or molecules preventing a sudden collapse [21, 22, 23] or by taking advantage of average results obtained from the diameter distribution found in ensemble samples. This represents a key field of study to broaden the scope of CNT uses and applications, calling for a real need to experimentally characterize the geometrical state of the carbon nanotube cross-section. Recently exciting new possibilities have emerged in the field of carbon nanotube spectroscopy, with the demonstration of the ability to identify between their circu-

*Corresponding author. E-mail address: alfonso.san-miguel@univ-lyon1.fr (A. San-Miguel).

lar or collapsed states using the Raman D-band [3]. The Raman D-band, or defect-band, is classically associated to the presence of defects in sp^2 carbon materials[24, 25, 26] but recent studies have shown that symmetry breaking can also lead to the development of this signature [3, 27]. By detecting collapsed tubes at ambient conditions, the D-band has already proven its interest for detecting intrinsically collapsed geometries due to large tube diameters. In this work, we show that this spectroscopic signature can be extended to further characterize progressive and reversible changes between the circular and collapsed states of the tube cross-section, opening up exciting opportunities for electro-optical engineering of nanotubes through their geometry. Tuning of the geometry is induced by applying high pressure, here in a sapphire anvil cell to open up the D-band spectroscopic window. We follow the collapse transition with the increasing D-Band intensity and demonstrate the reversibility of the process in the range of pressure explored. The study is performed on bundle samples and then applied to an individualized single wall nanotube, paving the way for the comprehensive investigation of the effects of intrinsic and environment configurations on the geometrical shape of carbon nanotubes.

2. Experimental methods

We performed high pressure experiments using a pressure device in opposed anvils geometry configuration as shown in Figure 1a. Diamond is the conventionally used anvil material, however it is not entirely suiting the study of CNTs due to its prominent Raman signal overlapping with the D-band. To overcome this issue, we used a sapphire anvils cell (SAC). In Figure 1b, typical Raman spectra of the sapphire and diamond anvils illustrate the clear spectroscopic window offered in the case of sapphire whereas the first order Raman peak of diamond largely overlaps with the Raman D-band of CNT. The main drawback of using sapphire anvils is given by the lower pressure they withstand before breaking when compared to the much harder diamond anvils. Here we could reach up to 4.2 GPa with no anvil failure using selected crystals and soft grade steel gaskets (steel T304). We adopted two different pressure transmitting media (PTM): Nitrogen (N_2) and an alcohol mixture of 4:1 methanol:ethanol (4:1 Me:Et), both presenting (quasi-) hydrostaticity in the studied pressure range [28]. We studied two kinds of single wall CNT (SWCNT) samples stemming from the same powder but differing in their density on the anvil surface: mixed bundles from direct powder grain deposition and more dispersed tubes from a drop casted solution (see SI). Raman spectra were obtained using a custom-made Raman spectrometer with 532 nm excitation source and an accuracy of 1 to 2 cm^{-1} (see SI).

3. Results and discussion

Figure 2 shows the pressure evolution of the D (~1350 cm^{-1}), G (~1600 cm^{-1}) and 2D-bands (~2700 cm^{-1}) of CNT bundles ensembles directly deposited on the anvil as dry powder grains (see SI). We observe the expected blue shift of the modes frequency with pressure. We emphasize the clearance of the anvil signal in the D-band region throughout the whole studied pressure range. We can record the increase of the D-band intensity relative to the G-band intensity during compression. This increase is found in both the Me:Et mix and N_2 experiments, indicating that the nature of the PTM has reduced impact on the CNT shape response. During the decompression cycle, in the N_2 experiment, the D-band relative intensity decreases upon pressure release returning to a similar value to that of the spectrum before the experiment. The pressure release cycle was not followed in the Me:Et experiment, yet the ambient pressure points recorded at the beginning and the end of the experiment (insets in Figure 2a and Figure 2c) agree with the D-band evolution reversibility. We interpret this result with a D-band originating from a defect-free scattering process as described in [3]. The successive collapse of the many CNTs in these bundle samples is responsible for the continuous increase of the D-band intensity throughout the compression. The reversibility of the tubes' collapse during the release cycle is also recorded. Interestingly, we observe a strong hysteresis in the process, with a slow decrease of D-band intensity until ~1 GPa followed by a sharp drop to reach back the initial state at the cell opening. This suggests that

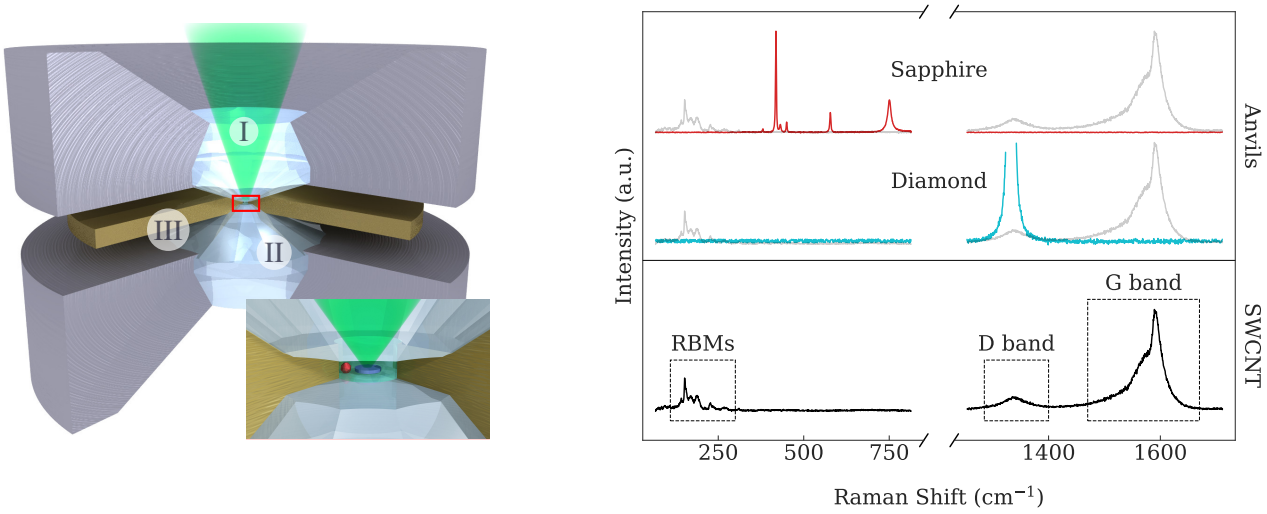

(a) (b)

Figure 1: (a) Schematic of the SAC. Highlighted are the probe laser beam (I) entering the sapphire anvil (II). The pair of anvils are compressing a metallic gasket (III) where a hole is drilled in order to form the compression chamber (red rectangle). The inset shows a zoom of the compression chamber. This area is filled with the PTM and it contains the samples and the ruby chips used for pressure measurements. (b) Superposition of the Raman signals of sapphire and diamond anvils (coloured spectra) over the Raman signal of SWCNT (black line) at ambient pressure. The spectra are normalized to show the typical intensities found in high pressure experiments.

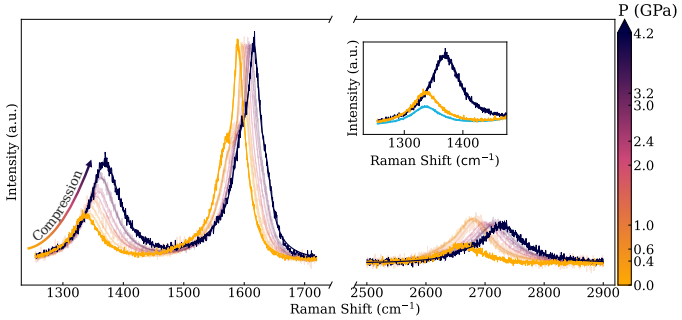

(a) Nitrogen PTM - Compression

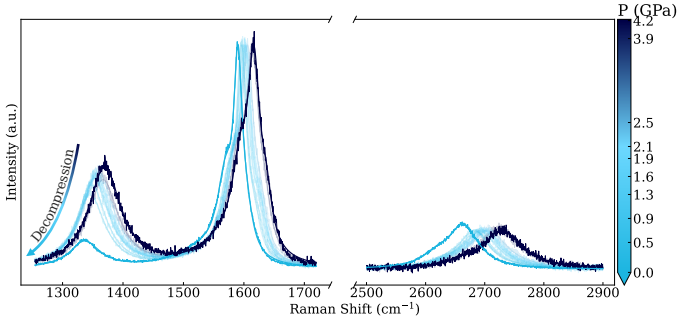

(b) Nitrogen PTM - Decompression

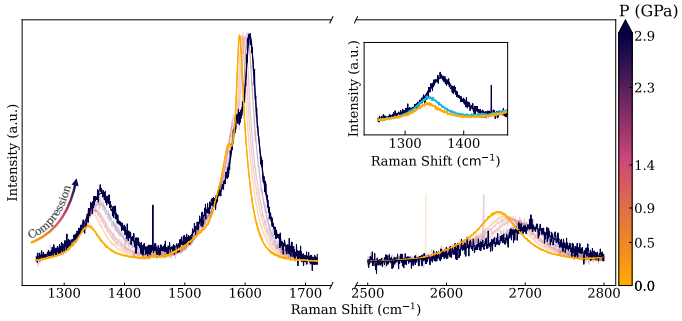

(c) 4:1 Methanol:Ethanol PTM

Figure 2: Pressure evolution of the D, G and 2D-bands for the bundles samples of the two experiments. In the nitrogen experiment both compression (a, left) and decompression (b, right) are shown. It has not been possible to record the decompression cycle for the alcohol experiment (c) so only the compression is shown. A color gradient bar shows the pressure values at which the spectra have been recorded. The insets show the D-band spectra obtained before and after the cycle, and at the maximum pressure for the two experiments. All the spectra are normalized to the G-band maximum value at each pressure point.

the nanotubes face difficulties to inflate back to their cylindrical geometry, stable at low pressure. Such difficulties may originate from the additional energy barrier introduced by the van der Waals interaction between walls in the nanotube collapsed state.

Supporting evidence towards our description of the phenomenon can be found when looking into the behaviour of the 2D-band. The latter is an interesting probe as it is not directly connected to the presence of defects in the sample. Moreover, modifications in the electronic structure induced by pressure which may affect the intensity of the D-band of the CNT's would similarly affect the 2D-band [29]. We observe in Figure 2 that the intensity of the 2D-band evolves in a completely different matter compared to that of the D-band. For what concerns the Nitrogen experiment we observe a rather flat response of its intensity with pressure both in the compression and decompression cycles. The initial spectrum at ambient pressure (Figure 2a) is the only spectrum featuring a considerably lower intensity. We must note, however, that this spectrum has been acquired before the PTM loading when the SWCNTs are subjected to different environmental conditions compared to the rest of the pressure run. In the Me:Et experiment (Figure 2c) we again find a dissimilar trend in the evolution of the 2D-band intensity when compared to that of the D-band. In this case, the 2D-band intensity is decreasing with pressure. The detailed description of the evolution of the 2D-band with pressure is beyond the scope of this paper. However, those evidence indicates that the origin of the increase of the D-band intensity can not be associated with electronic structure modification with pressure but rather a defect-free induced D-band due to the change in geometry of the CNTs.

To proceed further in the analysis, all the spectra are fitted using Lorentzian functions for both the D and G-bands (see SI). In the following, the ratio between the area below the D-band and the area below the G-band components, A_D/A_G, has been used to quantitatively follow the tubes' collapse. In Figure 3 we can find the evolution of A_D/A_G as a function of pressure which further illustrates the hysteresis cycle previously discussed. In addition to that we observe a sudden step in the A_D/A_G values during decompression, close to the solid-liquid N_2 PTM phase transition at 2.5 GPa. This may be associated with the collapse of those CNTs which were in a metastable state due to non-hydrostatic pressure in the solid phase. Previous high-pressure studies reported irreversible D-band changes in recovered samples compressed above 10 GPa. The origin of the D-band was attributed in this case to shear forces damaging the tubes at high pressure [30]. On the other hand, reversible changes in the D-band have been previously reported in axially strained carbon nanotubes up to 5% strain [27].

The nanotube's collapse can be cross checked using the RBM signal drop in intensity which has been reported and well characterized [31]. This was only possible using Me:Et as PTM due to the strong rotational spectrum of N_2 present in the RBM region. Figure 4a and Figure 4b show the pressure evolution of respectively the Raman spectrum and the peak integrated areas for the most prominent RBMs. For all diameters we find a first sudden intensity drop at the early stages of compression as previously reported [31]. The RBM area becomes then rather constant up to 1.4 GPa. Above this pressure RBM peaks corresponding to diameters from 1.4 to 1.7 nm disappear with only the 1 nm tube signal still present at the highest pressure. This threshold pressure of 1.4 GPa, attributed to the collapse of these SWCNTs, is compatible with the reported one in literature [31], beside the 1.4 nm tube which was expected, following a modified Levy-Carrier law [8], to collapse at slightly higher pressure (3.2 GPa). These correlated observations strengthen our interpretation of D-band intensity as a probe of the CNT changes in shape.

To complete the exploitation of the spectra, further analysis have been carried out on the pressure evolution of the bands frequency. The G^+-band shift with pressure in SWCNT have been extensively studied [22].The fitted D- and G-band positions as a function of pressure are presented in SI. We measured a linear G-band shift with pressure between $\sim$ 5 and $\sim$ 7.3 $cm^{-1}GPa^{-1}$ for the majority of the bands. Slightly higher slopes are observed when nitrogen was used as PTM when compared to alcohol as PTM. For what concerns the D-band pressure coefficient we obtain the comparable values of 7.4 ± 0.7 $cm^{-1}GPa^{-1}$ and 7.1 ± 0.1 $cm^{-1}GPa^{-1}$ for bundles in 4:1 Me:Et and nitrogen PTMs respectively.

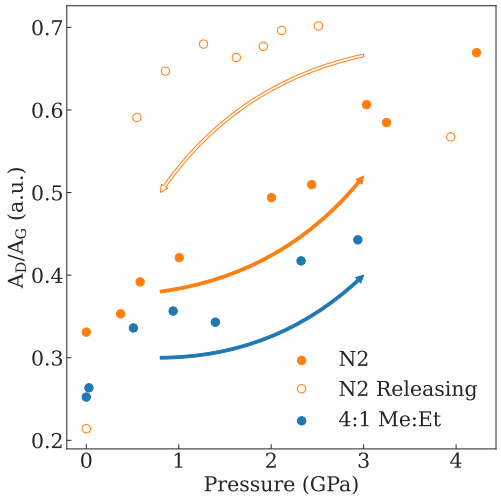

Figure 3: Pressure evolution of the ratio between the area of the D-band and the area of the G-band, A_D/A_G , for the experiments using dry transferred CNT bundles. Blue points show the data in the case of Methanol:Ethanol as PTM and orange in the case of Nitrogen. For the latter, solid points are acquired during compression and the empty ones during decompression. Lines are introduced as a guide to the eye.

These values can be compared with those found in literature for bundles of argon-filled tubes of 1.4 nm tubes which gave 5.5 $cm^{-1}GPa^{-1}$ for pressures beyond 15 GPa [13].

The use of nanotube bundles has the advantage of simple deposition and of giving an intense Raman signal due to the high number of probed tubes. On the other hand, this only allows a description of the average behaviour of the population of tubes present in the bundle. In particular, when dealing with the D-band, we have a weak dependency of its frequency with the nanotube diameter and thus all tubes contribute to the D-band signal. To characterize more accurately the geometrical transition introduced by the tube's collapse, we need to narrow down the distribution of probed SWCNTs going towards the study of individual SWCNT. This is experimentally very challenging in high pressure experiments due to the signal reduction introduced by the presence of the anvils and PTM in the optical path. We achieved the pressure study of a single chirality by dispersing the SWCNT powder in an organic solvent at a high dilution rate and drop casting the solution on the anvil surface (see SI). The most likeable assignment of the studied SWCNT chirality was identified as (16,8)

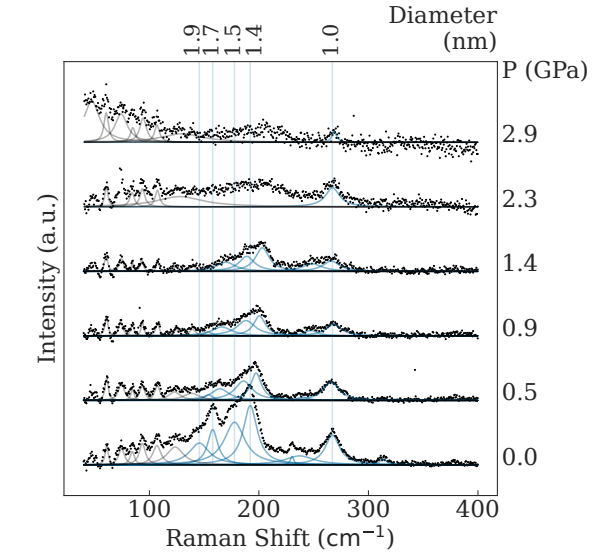

(a)

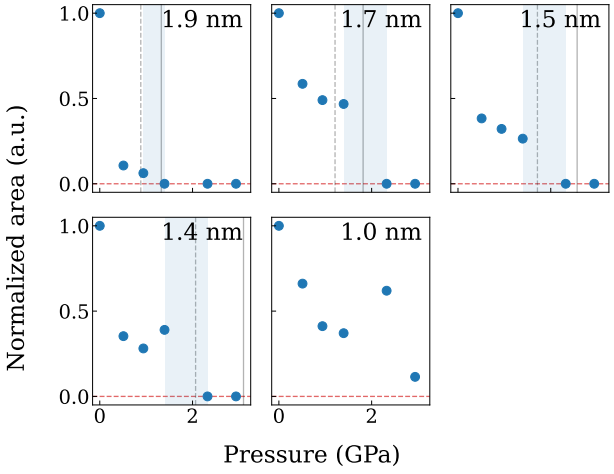

(b)

Figure 4: (a) Pressure evolution of the tubes' RBMs obtained during the experiment using 4:1 Me:Et as PTM. Lorentzian functions are used to fit the individual RBMs (blue lines) on the background subtracted data (black dots). The low frequency spectrum is polluted by the air rotational spectrum (grey lines). Additional blue vertical lines are added as a guide to the eye to match each RBM at ambient pressure with their diameter. (b) Blue dots show the evolution of the individual RBMs area with pressure. The area is normalized to the point at 0 GPa. A red horizontal line at zero intensity helps to visualize the disappearance of the RBMs. A light blue rectangle highlight the region where the intensity goes to zero. Gray dashed and solid vertical lines show the beginning and the end of the collapse calculated using the modified Levy-Carrier prediction [8].

by measuring the tube diameter using the RBM and matching it onto the excitonic Kataura plot [32] (see SI). The probed Raman signal can correspond to an isolated single or few tubes of the same chirality, or to a small isolated bundle comprising this chirality as the most optically resonant one.

The evolution of the G and D-band spectra with pressure for this sample is shown in Figure 5a. A clear transition is observed around 2 GPa. A drop in intensity of the overall signal is evidenced, marked by the increase of the signal to noise ratio as well as the relative augmentation of the intensity of the oxygen peaks around 1550 cm^{-1}. This can be related to the theoretically predicted modification in Raman signal that the nanotubes experience at collapse due to drastic modification of the electronic band structure [33]. The latter is also confirmed by the disappearance of the 2D-band at the same pressure (see Figure S4 in SI). In order to improve the quality of the data the acquisition time has been doubled for the spectra acquired at pressures higher then 2 GPa. The A_D/A_G ratio shown in Figure 5b experiences a change in behaviour between 1 and 2 GPa where after an initial flat response it rapidly increases until stabilizing to a higher value. We thus assigned those two thresholds of pressure to the beginning and the end of the collapse of this specific chirality. Between those two values the SWCNT undergoes a transient phase where it is found to be in an intermediate geometry. A small step increase is also observed around 0.4 GPa in A_D/A_G . The most probable origin of this increase is that a weakly resonant, larger diameter chirality, not identifiable in our RBM spectrum, is also present in the sample and partially contributes to the evolution of A_D/A_G with a collapse at low pressure.

The nature of the intermediate state cannot be defined from our results. The abundant modelling of the pressure induced radial collapse shows a number of intermediate states between the circular cross-section and the collapsed geometry including racetrack or polygonised shapes. Macroscopic models and molecular dynamics modelling in carbon nanotube bundles show that the collapse process extends in a large pressure domain in which mixed geometries can be found in the bundle [8].

Due to the impossibility of measuring the RBMs in this dispersed tubes experiment, a direct comparison with their signal is not possible. We could, however, extract the RBM intensity evolution corresponding to the (16,8) tube from the bundle experiment in Me:Et PTM and overlap it in Figure 5b. An excellent agreement in the measured collapse pressure is found using the two independent methods. The collapse region defined in Figure 5b also agrees with the modified Levy-Carrier prediction [8] which for a (16,8) tube gives an onset of the collapse pressure of 1.2±0.2 GPa and a collapse end of 1.8±0.2 GPa.

4. Conclusion

We performed high pressure studies on SWCNT bundles at high pressure using a sapphire anvil cell. This allowed us to follow the evolution of the tubes Raman D-band with pressure. This is a rarely studied feature of carbon based materials in high pressure experiments due to an important overlap with the diamond Raman signature, the latter being the most common material for the fabrication of high pressure anvils. Our study confirms that sapphire anvil cells are a powerful tool for the in-situ monitoring of structural modification of carbon-based materials. Our results show the appearance of a defect-free Raman D-band stemming from the CNT radial collapse with pressure. We find the process to be reversible leaving the samples undamaged after the pressure cycle in hydrostatic and quasi-hydrostatic pressure conditions. Our study provides a clear additional confirmation of the capability of using the Raman D-band to detect the collapsed geometry in carbon nanotubes [3]. Importantly, we performed studies on isolated CNTs which allowed us to follow the behaviour of a single chirality with pressure. This demonstrates the use of D-band as an efficient, fine new spectroscopic signature of the tube's progressive and reversible collapse with pressure, and more generally its geometrical state. It provides a direct proof of the collapse identified by the appearance of a new signature thus avoiding eventual problems connected to loss in signal, resonance or parasite background that might affect the usual RBMs analysis. This original probing method opens up new roads for the study of CNT shape evolution induced

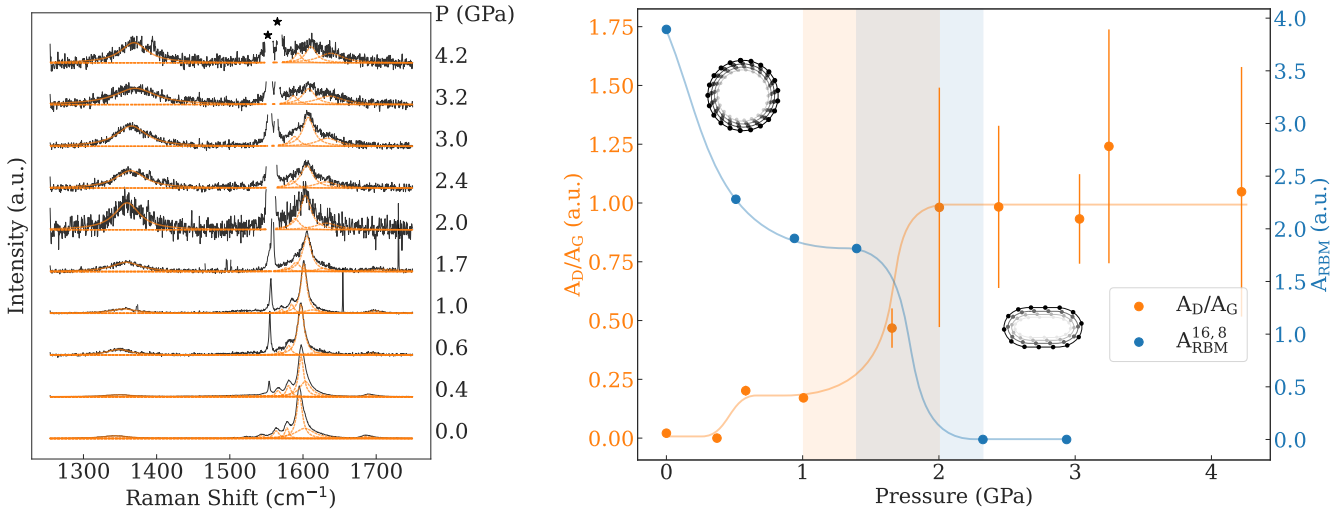

(a) (b)

Figure 5: (a) D and G-bands spectra evolution of the dispersed CNT with pressure. In orange are plotted the components of the D and G-bands fitting the data points in black. Two black stars highlight the dioxygen's Raman signals due to the presence of the molecule inside and outside the cell. (b) The orange dots show the evolution of the corresponding A_D/A_G as a function of pressure. The steep increase in the ratio noticed between 1 GPa and 2 GPa is highlighted by the light orange rectangle area. Overlapped, in blue, we find the plot of the (16,8) tube RBM's area as a function of pressure obtained in the Methanol:Ethanol experiment. A blue rectangle is highlighting the transition for this experiment. Orange and blue solid lines are used as guide to the eyes for the evolution of the data in the two cases.

by pressure, potentially resolved at the single nanotube scale to unveil chirality and local environment effects. This can foster theoretical studies to better understand the defect-free Raman D-band processes in relation to the cross-section shape and curvature of nanotubes.

Declaration of competing interest

The authors declare that they have no known competing financial interests or personal relationships that could have appeared to influence the work reported in this paper.

Acknowledgements

The authors acknowledge the support from ANR (project 2DPRESTO ANR-19-CE09-0027) and the CNRS High-Pressure Network (Initiative Développement Technologiques 2020 program).

References

[1] O. Arroyo-Gascón, R. Fernández-Perea, E. S. Morell, C. Cabrillo, L. Chico, Universality of moiré physics in collapsed chiral carbon nanotubes, Carbon 205 (2023) 394–401. doi:https://doi.org/10.1016/j.carbon.2023.01.052.
URL https://www.sciencedirect.com/science/article/pii/S0008622323000593

[2] C. Miralaei, S. L. Floch, R. Debord, H. V. Nguyen, J. C. D. Silva, A. San-Miguel, H. L. Poche, S. Pailhès, V. Pischedda, Effect of extreme mechanical densification on the electrical properties of carbon nanotube micro-yarns, Nanotechnology 33 (27) (2022) 275708. doi:10.1088/1361-6528/ac6039.
URL https://dx.doi.org/10.1088/1361-6528/ac6039

[3] E. Picheau, A. Impellizzeri, D. Rybkovskiy, M. Bayle, J.-Y. Mevellec, F. Hof, H. Saadaoui, L. Noé, A. C. Torres Dias, J.-L. Duvail, M. Monthioux, B. Humbert, P. Puech, C. P. Ewels, A. Pénicaud, Intense raman d band without disorder in flattened carbon nanotubes, ACS Nano 15 (1) (2021) 596–603, pMID: 33444504. arXiv:https://doi.org/10.1021/acsnano.0c06048, doi:10.1021/acsnano.0c06048.
URL https://doi.org/10.1021/acsnano.0c06048

[4] D. H. Choi, Q. Wang, Y. Azuma, Y. Majima, J. H. Warner, Y. Miyata, H. Shinohara, R. Kitaura, Fabrication and characterization of fully flattened carbon nanotubes: A new graphene nanoribbon analogue, Scientific Reports 3 (2013).

[5] M. S. C. Mazzoni, H. Chacham, Bandgap closure of a flat-

tened semiconductor carbon nanotube: A first-principles study, Applied Physics Letters 76 (12) (2000) 1561–1563. arXiv:https://doi.org/10.1063/1.126096, doi:10.1063/1.126096.
URL https://doi.org/10.1063/1.126096

[6] T. W. Tombler, C. Zhou, J. Kong, H. Dai, Gating individual nanotubes and crosses with scanning probes, Applied Physics Letters 76 (17) (2000) 2412–2414. arXiv:https://doi.org/10.1063/1.125611, doi:10.1063/1.125611.
URL https://doi.org/10.1063/1.125611

[7] R. B. Capaz, C. D. Spataru, P. Tangney, M. L. Cohen, S. G. Louie, Hydrostatic pressure effects on the structural and electronic properties of carbon nanotubes, Phys. Status Solidi B 241 (14) (2004) 3352–3359. doi:10.1002/pssb.200490021.

[8] Y. Magnin, F. Rondepierre, W. Cui, D. Dunstan, A. San-Miguel, Collapse phase diagram of carbon nanotubes with arbitrary number of walls. collapse modes and macroscopic analog, Carbon 178 (2021) 552–562. doi:https://doi.org/10.1016/j.carbon.2021.03.031.

[9] J. A. Elliott, J. K. W. Sandler, A. H. Windle, R. J. Young, M. S. P. Shaffer, Collapse of Single-Wall Carbon Nanotubes is Diameter Dependent, Phys. Rev. Lett. 92 (9) (2004) 095501. doi:10.1103/PhysRevLett.92.095501.

[10] P. Tangney, R. B. Capaz, C. D. Spataru, M. L. Cohen, S. G. Louie, Structural transformations of carbon nanotubes under hydrostatic pressure, Nano Lett. 5 (11) (2005) 2268–2273. doi:10.1021/nl051637p.

[11] S. Zhang, R. Khare, T. Belytschko, K. J. Hsia, S. L. Mielke, G. C. Schatz, Transition states and minimum energy pathways for the collapse of carbon nanotubes, Phys. Rev. B 73 (2006) 075423. doi:https://doi.org/10.1103/PhysRevB.73.075423.

[12] A. L. Aguiar, E. B. Barros, R. B. Capaz, A. G. Souza Filho, P. T. C. Freire, J. Mendes Filho, D. Machon, C. Caillier, Y. A. Kim, H. Muramatsu, M. Endo, A. San-Miguel, Pressure-induced collapse in double-walled carbon nanotubes: Chemical and mechanical screening effects, J. Phys. Chem. C 115 (13) (2011) 5378–5384.

[13] A. Merlen, N. Bendiab, P. Toulemonde, A. Aouizerat, A. San Miguel, J. L. Sauvajol, G. Montagnac, H. Cardon, P. Petit, Resonant raman spectroscopy of single-wall carbon nanotubes under pressure, Phys. Rev. B 72 (2005) 035409. doi:10.1103/PhysRevB.72.035409.

[14] M. Yao, Z. Wang, B. Liu, Y. Zou, S. Yu, W. Lin, Y. Hou, S. Pan, M. Jin, B. Zou, T. Cui, G. Zou, B. Sundqvist, Raman signature to identify the structural transition of single-wall carbon nanotubes under high pressure, Phys. Rev. B 78 (20) (2008) 205411. doi:10.1103/PhysRevB.78.205411.

[15] A. J. Ghandour, D. J. Dunstan, A. Sapelkin, G-mode behaviour of closed ended single wall carbon nanotubes under pressure, physica status solidi (b) 246 (3) (2009) 491–495.

[16] R. S. Alencar, A. L. Aguiar, A. R. Paschoal, P. T. C. Freire, Y. A. Kim, H. Muramatsu, M. Endo, H. Terrones, M. Terrones, A. San-Miguel, M. S. Dresselhaus, A. G. Souza Filho, Pressure-induced selectivity for probing inner tubes in double- and triple-walled carbon nanotubes: A resonance raman study, J. Phys. Chem. C 118 (15) (2014) 8153–8158.

[17] F. Balima, S. L. Floch, C. Adessi, T. F. Cerqueira, N. Blanchard, R. Arenal, A. Brûlet, M. A. Marques, S. Botti, A. San-miguel, Radial collapse of carbon nanotubes for conductivity optimized polymer composites, Carbon 106 (2016) 64 – 73.

[18] R. S. Alencar, W. Cui, A. C. Torres-Dias, T. F. T. Cerqueira, S. Botti, M. A. L. Marques, O. P. Ferreira, C. Laurent, A. Weibel, D. Machon, D. J. Dunstan, A. G. S. Filho, A. San-Miguel, Pressure-induced radial collapse in few-wall carbon nanotubes: A combined theoretical and experimental study, Carbon 125 (2017) 429 – 436. doi:10.1016/j.carbon.2017.09.044.

[19] S. Silva-Santos, R. Alencar, A. Aguiar, Y. Kim, H. Muramatsu, M. Endo, N. Blanchard, A. San-Miguel, A. Souza Filho, From high pressure radial collapse to graphene ribbon formation in triple-wall carbon nanotubes, Carbon 141 (2019) 568–579. doi:https://doi.org/10.1016/j.carbon.2018.09.076.
URL https://www.sciencedirect.com/science/article/pii/S0008622318308923

[20] D. Machon, V. Pischedda, S. Le Floch, A. San-Miguel, Perspective: High pressure transformations in nanomaterials and opportunities in material design, Journal of Applied Physics 124 (16) (2018) 160902. arXiv:https://pubs.aip.org/aip/jap/article-pdf/doi/10.1063/1.5045563/15217382/160902_1_online.pdf, doi:10.1063/1.5045563.
URL https://doi.org/10.1063/1.5045563

[21] L. Alvarez, J.-L. Bantignies, R. Le Parc, R. Aznar, J.-L. Sauvajol, A. Merlen, D. Machon, A. San Miguel, High-pressure behavior of polyiodides confined into single-walled carbon nanotubes: A raman study, Phys. Rev. B 82 (2010) 205403.

[22] A. C. Torres-Dias, S. Cambré, W. Wenseleers, D. Machon, A. San-Miguel, Chirality-dependent mechanical response of empty and water-filled single-wall carbon nanotubes at high pressure, Carbon 95 (2015) 442–451. doi:https://doi.org/10.1016/j.carbon.2015.08.032.
URL https://www.sciencedirect.com/science/article/pii/S0008622315301512

[23] C. Bousige, A. Stolz, S. D. Silva-Santos, J. Shi, W. Cui, C. Nie, M. A. Marques, E. Flahaut, M. Monthioux, A. San-Miguel, Superior carbon nanotube stability by molecular filling:a single-chirality study at extreme pressures, Carbon 183 (2021) 884–892. doi:https://doi.org/10.1016/j.carbon.2021.07.068.
URL https://www.sciencedirect.com/science/article/pii/S0008622321007521

[24] M. S. Dresselhaus, A. Jorio, A. G. Souza Filho, R. Saito, Defect characterization in graphene and carbon nanotubes using raman spectroscopy, Philosophical Transactions of the Royal Society A: Mathematical, Physical and Engineering Sciences 368 (1932) (2010) 5355–5377. arXiv:https://royalsocietypublishing.org/doi/pdf/10.1098/rsta.2010.0213, doi:10.1098/rsta.2010.0213.
URL https://royalsocietypublishing.org/doi/abs/10.1098/rsta.2010.0213

[25] L. G. Cançado, M. G. da Silva, E. H. M. Ferreira, F. Hof, K. Kampioti, K. Huang, A. Pénicaud, C. A. Achete, R. B. Capaz, A. Jorio, Disentangling contributions of point and line defects in the raman spectra of graphene-related materials, 2D Materials 4 (2) (2017) 025039. doi:10.1088/2053-1583/aa5e77.
URL https://dx.doi.org/10.1088/2053-1583/aa5e77

[26] R. Beams, L. G. Cançado, L. Novotny, Raman characterization of defects and dopants in graphene, Journal of Physics: Condensed Matter 27 (8) (2015) 083002. doi:10.1088/0953-8984/27/8/083002.
URL https://dx.doi.org/10.1088/0953-8984/27/8/083002

[27] C.-C. Chang, C.-C. Chen, W.-H. Hung, I. K. Hsu, M. A. Pimenta, S. B. Cronin, Strain-induced d band observed in carbon nanotubes, Nano Research 5 (12) (2012) 854–862. doi:10.1007/s12274-012-0269-3.
URL https://doi.org/10.1007/s12274-012-0269-3

[28] S. Klotz, J.-C. Chervin, P. Munsch, G. L. Marchand, Hydrostatic limits of 11 pressure transmitting media, Journal of Physics D: Applied Physics 42 (7) (2009) 075413. doi:10.1088/0022-3727/42/7/075413.
URL https://dx.doi.org/10.1088/0022-3727/42/7/075413

[29] M. Dresselhaus, G. Dresselhaus, R. Saito, A. Jorio, Raman spectroscopy of carbon nanotubes, Physics Reports 409 (2) (2005) 47–99. doi:https://doi.org/10.1016/j.physrep.2004.10.006.
URL https://www.sciencedirect.com/science/article/pii/S0370157304004570

[30] A. Merlen, P. Toulemonde, S. Le Floch, G. Montagnac, T. Hammouda, O. Marty, A. San Miguel, High pressure–high temperature synthesis of diamond from single-wall pristine and iodine doped carbon nanotube bundles, Carbon 47 (7) (2009) 1643–1651. doi:https://doi.org/10.1016/j.carbon.2009.02.014.
URL https://www.sciencedirect.com/science/article/pii/S0008622309000918

[31] A. C. Torres-Dias, T. F. Cerqueira, W. Cui, M. A. Marques, S. Botti, D. Machon, M. A. Hartmann, Y. Sun, D. J. Dunstan, A. San-Miguel, From mesoscale to nanoscale mechanics in single-wall carbon nanotubes, Carbon 123 (2017) 145–150. doi:https://doi.org/10.1016/j.carbon.2017.07.036.
URL https://www.sciencedirect.com/science/article/pii/S0008622317307194

[32] A. R. T. Nugraha, R. Saito, K. Sato, P. T. Araujo, A. Jorio, M. S. Dresselhaus, Dielectric constant model for environmental effects on the exciton energies of single wall carbon nanotubes, Applied Physics Letters 97 (9) (2010) 091905. arXiv:https://pubs.aip.org/aip/apl/article-pdf/doi/10.1063/1.3485293/14437448/091905_1_online.pdf, doi:10.1063/1.3485293.
URL https://doi.org/10.1063/1.3485293

[33] A. L. Aguiar, R. B. Capaz, A. G. Souza Filho, A. San-Miguel, Structural and phonon properties of bundled single- and double-wall carbon nanotubes under pressure, The Journal of Physical Chemistry C 116 (42) (2012) 22637–22645. arXiv:https://doi.org/10.1021/jp3093176, doi:10.1021/jp3093176.
URL https://doi.org/10.1021/jp3093176